

# MicroRNA-sensitive Oncolytic Measles Viruses for Cancer-specific Vector Tropism

Mathias F Leber<sup>1</sup>, Sascha Bossow<sup>1</sup>, Vincent HJ Leonard<sup>2</sup>, Karim Zaoui<sup>1</sup>, Christian Grossardt<sup>1</sup>, Marie Frenzke<sup>2</sup>, Tanner Miest<sup>2</sup>, Stefanie Sawall<sup>1</sup>, Roberto Cattaneo<sup>2</sup>, Christof von Kalle<sup>1</sup> and Guy Ungerechts<sup>1</sup>

<sup>1</sup>Department of Translational Oncology, National Center for Tumor Diseases (NCT) and German Cancer Research Center (DKFZ), Heidelberg, Germany; <sup>2</sup>Department of Molecular Medicine and Virology and Gene Therapy Track, Mayo Clinic College of Medicine, Rochester, Minnesota, USA

Oncolytic measles viruses (MV) derived from the live attenuated vaccine strain have been engineered for increased tumor-cell specificity, and are currently under investigation in clinical trials including a phase I study for glioblastoma multiforme (GBM). Recent preclinical studies have shown that the cellular tropism of several viruses can be controlled by inserting microRNA-target sequences into their genomes, thereby inhibiting spread in tissues expressing cognate microRNAs. Since neuron-specific microRNA-7 is downregulated in gliomas but highly expressed in normal brain tissue, we engineered a microRNA-sensitive virus containing target sites for microRNA-7 in the 3'-untranslated region of the viral fusion gene. In presence of microRNA-7 this modification inhibits translation of envelope proteins, restricts viral spread, and progeny production. Even though highly attenuated in presence of microRNA-7, this virus retained full efficacy against glioblastoma xenografts. Furthermore, microRNA-mediated inhibition protected genetically modified mice susceptible to MV infection from a potentially lethal intracerebral challenge. Importantly, endogenous microRNA-7 expression in primary human brain resections tightly restricted replication and spread of microRNA-sensitive virus. This is proof-of-concept that tropism restriction by tissue-specific microRNAs can be adapted to oncolytic MV to regulate viral replication and gene expression to maximize tumor specificity without compromising oncolytic efficacy.

Received 3 November 2010; accepted 16 February 2011; published online 5 April 2011. doi:10.1038/mt.2011.55

## INTRODUCTION

Many different families of viruses have been tested preclinically for oncolytic efficacy, and multiple viruses have emerged as promising cancer therapeutics that have made the transition into the clinic. In particular, measles virus (MV) has proven to be a viral vector platform with broad utility, having been developed for the treatment of several types of cancer in preclinical settings, and

clinical trials including phase I studies for treatment of ovarian cancer, myeloma, and recurrent glioma.<sup>1-4</sup>

Although safety is the main concern in the beginning of early clinical trials, efficacy is the key issue facing the development of the next generation of oncolytic viruses, including MV. One method of increasing antitumor activity is by incorporating suicide genes into the genome,<sup>5,6</sup> or by transient suppression of the immune response to viral infection.<sup>5,7,8</sup> Although these strategies generally produce more potent oncolysis, they may also increase toxic side effects, possibly decreasing the therapeutic index. Particularly, in an approach of chemotherapy-induced transient immunosuppression there might be an increased risk of uncontrolled virus replication. Therefore, application of immunosuppression in future virotherapy clinical trials depends on tight control over virus replication, especially in the treatment of sensitive tissue like brain, to ensure that efficacy can be maximized without risking virus replication in nontarget tissue.

To control tissue tropism of oncolytic viruses, tissue-specific expression of cellular microRNAs has been exploited.<sup>9-13</sup> MicroRNAs are small (~20–23 nt) endogenous RNAs that are known to play important regulatory roles in cell proliferation, cell differentiation, apoptosis, and tumorigenesis by binding to the 3'-untranslated region (UTR) of the targeted mRNAs, thereby promoting either mRNA cleavage or repression of gene expression at the post-transcriptional level. Differential microRNA expression is a hallmark of cancer cells, with various microRNAs downregulated in malignant cells. Therefore, low expression of distinct microRNAs represents a common and specific characteristic of cancer cells that can be exploited by engineering microRNA-sensitive oncolytic viruses. To date, feasibility of microRNA-based regulation of oncolytic viruses has already been shown for vesicular stomatitis-, adeno-, coxsackie- and herpes simplex virus.<sup>9-13</sup> Recently, it was shown that miR7 is downregulated in glioblastoma multiforme (GBM), possibly contributing to uncontrolled tumor growth through upregulated expression of epidermal growth factor receptor, a target of miR7.<sup>14,15</sup> Both, this differential expression of miR7 between GBM and normal brain tissue and its fully conserved sequence between mouse and men makes this microRNA an excellent target for restricting oncolytic virus replication to neoplastic tissue. Besides its high abundance in the neuronal tissues, miR7 is also expressed

**Correspondence:** Guy Ungerechts, Department of Translational Oncology, National Center for Tumor Diseases (NCT), German Cancer Research Center (DKFZ), Im Neuenheimer Feld 460, D-69120 Heidelberg, Germany. E-mail: [guy.ungerechts@nct-heidelberg.de](mailto:guy.ungerechts@nct-heidelberg.de)

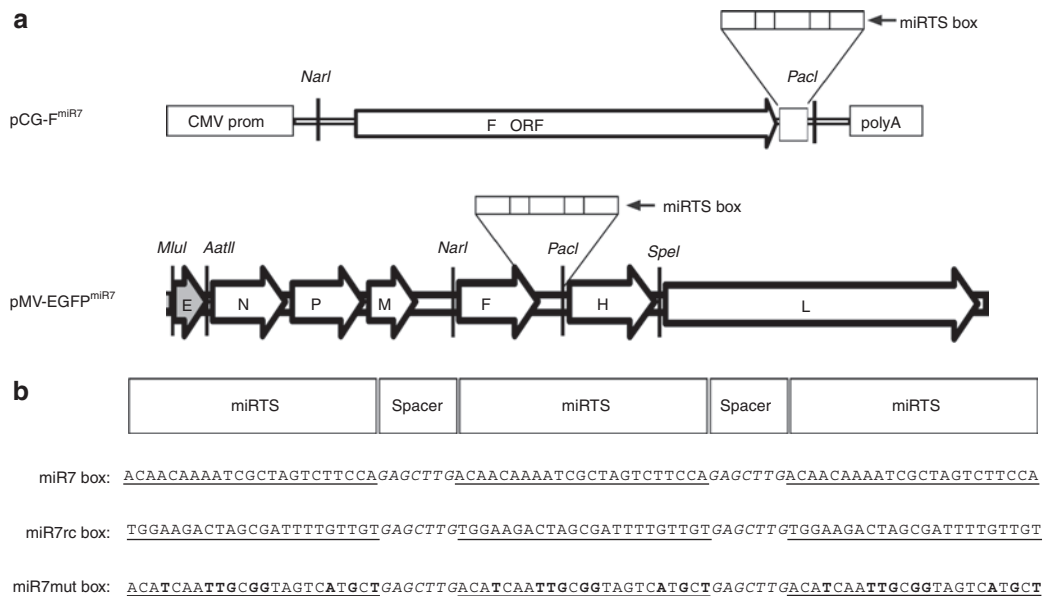


**Figure 1** Genome structure of the microRNA-sensitive measles virus. **(a)** Schematic illustration of the miR7-sensitive measles virus (MV) genome as well as the pCG-F<sup>miR7</sup> expression plasmid containing the microRNA-target site (miRTS) box in the 3'UTR of the F gene. The miRTS box was designed to be active in the mRNA of the F gene. In the MV-EGFP<sup>miR7</sup> genome, an additional transcription unit encoding the reporter EGFP was inserted upstream of the N gene. **(b)** Three different miRTS boxes containing three tandem copies each of a sequence with varying complementarity to the mature miR7 sequence separated by heptanucleotide spacers were constructed. The miR7 box shows high complementarity to miR7, whereas the miR7rc or miR7mut boxes contain the reverse complementary (rc) or mutated (mut) target sequence and should thus be nonfunctional. The microRNA-target sequences are underlined; mutated nucleotides of the miR7mut box are displayed bold.

in pituitary gland.<sup>16</sup> Because MV has a negative-sense, single-stranded RNA genome that is cotranscriptionally encapsidated,<sup>17</sup> the genome and the antigenome are both protected from the RNAi machinery by viral nucleocapsid proteins. Hence, we decided to target the mRNA of the viral fusion (F) gene by inserting miR7 target sites into its 3'UTR. By engineering the F mRNA to be sensitive toward miR7, a structural component of the virion is targeted and the late stage of infection is blocked. Moreover, targeting the F mRNA enables functional testing of the system already on plasmid level by means of the fusion assay.<sup>18-20</sup>

In this study, we engineered an oncolytic MV for glioma virotherapy regulated by a neuron-specific microRNA. MV expressing this modification retained full efficacy against GBM xenografts and protected genetically modified mice susceptible to MV infection from a potentially lethal intracerebral challenge. Importantly, endogenous microRNA-7 expression in primary human brain resections tightly restricted replication and spread of this microRNA-sensitive virus. This work is proof-of-concept that microRNA regulation of viral replication and gene expression can be adapted broadly to MV vectors potentially maximizing safety and antitumor activity of this vector system.

**RESULTS**

**Fusion activity of MV F<sup>miR7</sup> is regulated by miR7**

The structure of the viral RNA genome of recombinant MV vaccine strain containing the microRNA-target site (miRTS) box in the 3'UTR of the fusion (F) gene is depicted schematically in **Figure 1a**. To test the regulation of F mRNA by miR7, we generated an expression plasmid containing the modified fusion gene under transcriptional control of the CMV promoter, as shown in **Figure 1a**. Besides

the miR7 miRTS box, which includes three tandem copies of a sequence complementary to miR7 separated by heptanucleotide spacers (**Figure 1b**), we generated a reverse complementary target sequence (miR7rc), and a mutated one (miR7mut) with imperfect complementarity to the mature miR7 microRNA (**Figure 1b**). Functional activity of F protein after plasmid-mediated expression, as assessed by the previously described fusion assay,<sup>18-20</sup> revealed that the modified F protein coexpressed with the unmodified H protein induced syncytia formation in Vero cells equivalent to the positive control, whereas in the presence of co-transfected miR7 precursors, syncytia formation was completely inhibited (**Figure 2a**). In this experimental setting, both the miR7rc and miR7mut sequences served as negative controls, demonstrating no detectable inhibition of cell fusion in presence of miR7 due to noncomplementarity to the mature miR7 microRNA (**Figure 2a**).

We then assessed whether the observed sensitivity toward miR7 was, as hypothesized, due to a translational repression of the targeted F protein. We harvested cell lysates from fusion assays performed in presence of miR7 and immunoblotted against H and F. Translation of the F<sup>miR7</sup> mRNA containing synthetic miR7 target sequences was strongly reduced in presence of cognate microRNA, whereas translation of F<sup>miR7rc</sup> or F<sup>miR7mut</sup> transcripts remained unchanged (**Figure 2b**). Because both controls were equally unresponsive to the presence of mature miR7, we retained only miR7rc as a negative control for further analyses.

**MV accommodates microRNA-target elements without slowing of growth kinetics**

We next incorporated the modified F<sup>miR7</sup> or F<sup>miR7rc</sup> genes into the full-length MV genomes. All viruses could be rescued and amplified on

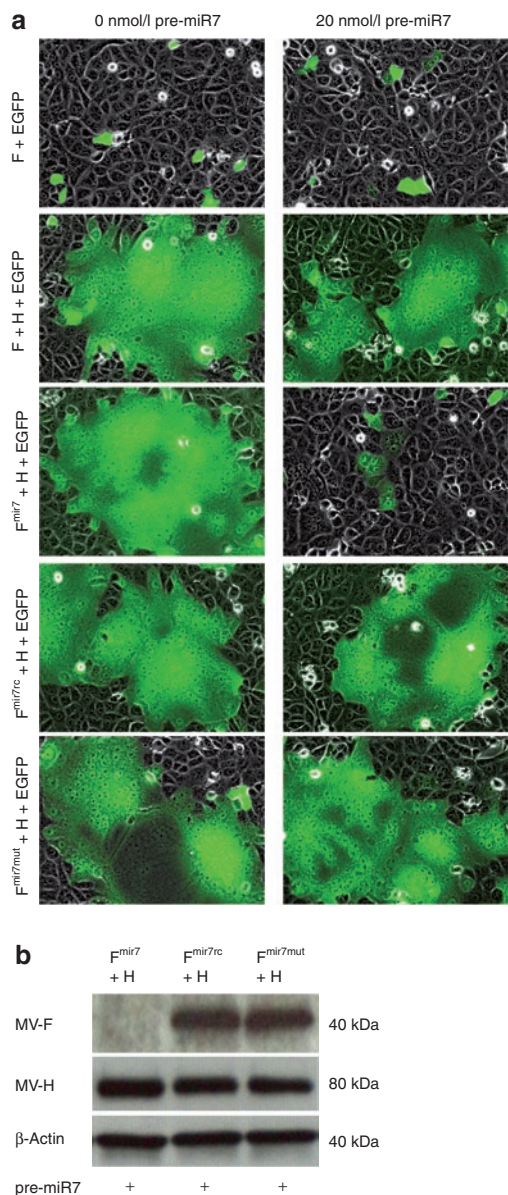


**Figure 2** Syncytia formation and expression of the measles virus (MV) *F* gene containing microRNA-target sites are repressed by the presence of miR7. **(a)**  $2 \times 10^5$  Vero cells/well were seeded in 12-well plates and after attachment co-transfected with 0 or 20 nmol/l of miR7 precursors along with different combinations of expression vectors encoding the reporter enhanced green fluorescent protein (EGFP), and viral *F* variants and *H* (fusion assay). Coexpression of the *F* and *H* gene is sufficient for inducing the typical, syncytial cytopathic effect of MV infection. Fluorescence and phase contrast microscopy pictures were taken 14 hours post-transfection ( $\times 200$  magnification). **(b)** Immunoblot analysis of protein lysates derived from Vero cells co-transfected with 800 ng each of the reporter EGFP, and viral *H* and *F* variants in presence of 20 nmol/l miR7 precursors. Cells were lysed 16 hours post-transfection, total protein was isolated and immunoblotted for *H*, *F*, and  $\beta$ -actin.

Vero cells. Integrity of the genomic structure and sequence identity of the inserted miRTS boxes were verified by RT-PCR using viral particles from the 3rd passage. Sequencing showed no alterations in the respective target sites demonstrating the genetic stability of introduced elements. The viruses were designated MV-EGFP<sup>miR7</sup> and MV-EGFP<sup>miR7rc</sup>, respectively. In order to assess their infectivity

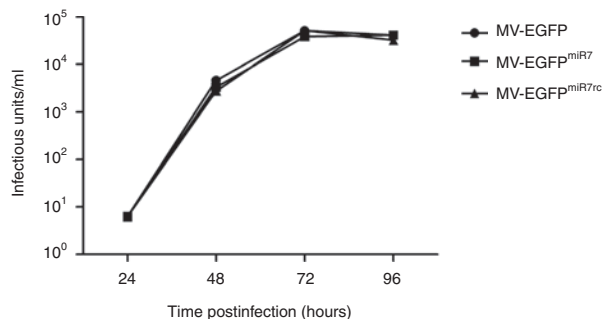


**Figure 3** Insertion of different microRNA-target site (miRTS) boxes does not alter viral replication kinetics. Multistep growth curves of the parental Edmonston-B vaccine strain virus and the recombinant viruses containing miRTS-boxes. U87 glioblastoma cells were infected with either MV-EGFP or the recombinant MV-EGFP<sup>miR7</sup>/MV-EGFP<sup>miR7rc</sup> at multiplicity of infection (MOI) of 0.03. Progeny virus particles were determined at the designated time points in octuplicate by serial-dilution titration assay on Vero cells. 72 hours postinfection, MV-EGFP had replicated to a titer of  $5.13 \times 10^4$  infectious units/ml, MV-EGFP<sup>miR7</sup> to  $3.88 \times 10^4$  infectious units/ml and MV-EGFP<sup>miR7rc</sup> to  $5.19 \times 10^4$  infectious units/ml.

and viability in target cells, we performed multistep and one-step growth curves with MV-EGFP<sup>miR7</sup>, MV-EGFP<sup>miR7rc</sup>, and the unmodified parental virus MV-EGFP on U87 glioblastoma cells (**Figure 3** and **Supplementary Figure S1**). All viruses showed comparable growth kinetics and replicated to similar titers.

### Attenuation of viruses containing miR7 complementary sequences in the presence of exogenous miR7

To determine the responsiveness of MV-EGFP<sup>miR7</sup> and MV-EGFP<sup>miR7rc</sup> to miR7, we transfected miR7 precursor molecules (pre-miR7) into Vero cells and subsequently infected them with either MV-EGFP<sup>miR7</sup> or MV-EGFP<sup>miR7rc</sup> at a multiplicity of infection (MOI) of 0.03. The pre-miR7 concentration of 20 nmol/l had been previously determined in a dose-escalation experiment (data not shown). The spread and fusogenicity of the viruses were analyzed by phase contrast and fluorescence microscopy (**Figure 4a**). In the absence of miR7, no difference in viral spread and syncytia formation could be detected after infection with MV-EGFP<sup>miR7</sup> or MV-EGFP<sup>miR7rc</sup>. In contrast, MV-EGFP<sup>miR7</sup>, containing miRTS complementary to miR7, was highly attenuated in terms of fusion and cell killing in the presence of miR7, whereas MV-EGFP<sup>miR7rc</sup> was unaffected by expression of miR7. This indicates that oncolytic MV can be engineered to be sensitive to the presence of a selected microRNA species.

To define whether the microRNA-based attenuation protects infected cells from virus-mediated cellular toxicity, we determined the cell viability of mock-infected, MV-EGFP<sup>miR7</sup>, or MV-EGFP<sup>miR7rc</sup>-infected cells in the absence or presence of miR7 precursors using a cell viability assay (**Figure 4b**). In the absence of microRNA, infections with both viruses resulted in a drop in cell viability to  $\sim 10\%$  of uninfected controls. However, when the cells had been previously transfected with miR7 precursors, cell viability was restored to  $\sim 90\%$  after infection with microRNA-sensitive MV-EGFP<sup>miR7</sup>, whereas the cytotoxicity of MV-EGFP<sup>miR7rc</sup> was unaffected.



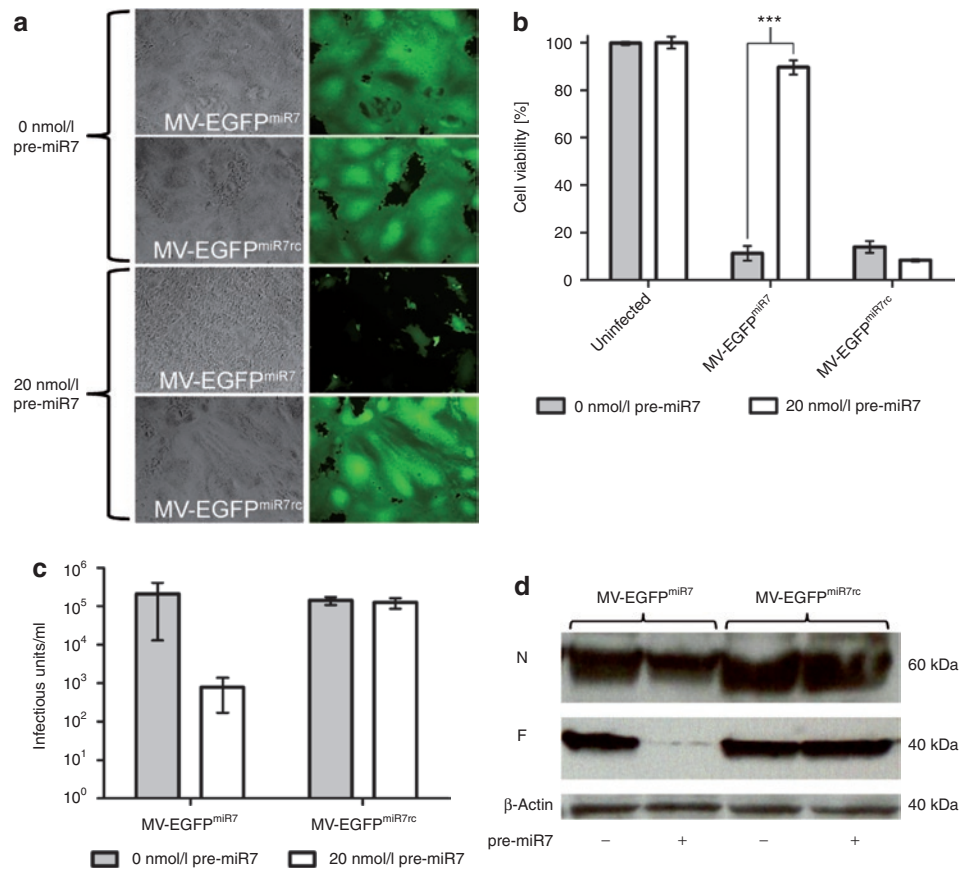


**Figure 4** miR7 regulates spreading, cytotoxicity, protein expression, and progeny virus production of MV-EGFP<sup>miR7</sup>. **(a)** Vero cells were seeded in 6-well plates at a density of  $6 \times 10^5$  cells/well. After attachment, cells were transfected with 0 or 20 nmol/l miR7 precursors and subsequently infected with MV-EGFP<sup>miR7</sup> or MV-EGFP<sup>miR7rc</sup> at a multiplicity of infection (MOI) of 0.03. Forty hours postinfection, fluorescence microscopy was performed in order to detect progeny virus production and spread throughout the cell layer ( $\times 100$  magnification). **(b)** Vero cells were seeded in 24-well plates at a density of  $4 \times 10^4$  cells/well. Cells were transfected with 0 or 20 nmol/l of miR7 precursor molecules and infected subsequently with MV-EGFP<sup>miR7</sup> or MV-EGFP<sup>miR7rc</sup> at an MOI of 0.03 followed by the XTT cell viability assay 87 hours postinfection. Statistical significance was tested using the two-tailed *t*-test. *P* values of  $<0.0001$  are indicated with three asterisks. **(c)** Vero cells were seeded in 12-well plates at a density of  $1.5 \times 10^5$  cells/well. After attachment, cells were transfected with either 0 or 20 nmol/l miR7 precursor molecules. Transfected cells were infected with MV-EGFP<sup>miR7</sup> or MV-EGFP<sup>miR7rc</sup> at an MOI of 0.03. Forty-eight hours postinfection, the cells were scraped in their medium, subjected to one freeze-thaw cycle and progeny virus titers were determined. **(d)** Immunoblot of protein lysates derived from Vero cells infected with MV-EGFP<sup>miR7</sup> or MV-EGFP<sup>miR7rc</sup> at an MOI of 0.03 in either the absence or presence of 20 nmol/l miR7 precursor molecules. Twenty-six hours postinfection cells were lysed, total protein was isolated and immunoblotted for  $\beta$ -actin, MV-N, and MV-F.

Next, we analyzed whether and to which extent virus progeny production is affected by miR7. To this end, we determined MV-EGFP<sup>miR7</sup> and MV-EGFP<sup>miR7rc</sup> progeny virus production in presence or absence of miR7 by titration analysis. In the case of the microRNA-responsive MV-EGFP<sup>miR7</sup>, we observed a reduction of the viral titer by more than two orders of magnitude, precisely 266-fold, in the presence of miR7 (Figure 4c). Control virus titers were not affected by microRNA presence.

After demonstrating that miR7 can negatively regulate production of infectious virus particles, we determined whether the mechanism of attenuation of MV-EGFP<sup>miR7</sup> is decreased expression of F protein. Mock or pre-miR7 transfected Vero cells were subsequently infected with MV-EGFP<sup>miR7</sup> or MV-EGFP<sup>miR7rc</sup> at an MOI of 0.03. F protein-specific immunoblotting revealed that the presence of miR7 strongly interfered with F protein expression specifically in cells infected with MV-EGFP<sup>miR7</sup>, whereas no difference could be detected in cells infected with MV-EGFP<sup>miR7rc</sup>

(Figure 4d). N protein levels were not significantly altered by the presence of miR7.

### MicroRNA-sensitive MV-EGFP<sup>miR7</sup> retains oncolytic efficacy in brain cancer cells

Next, we tested whether MV-EGFP<sup>miR7</sup> retains full efficacy against glioblastoma cells *in vitro*. Therefore, we infected U87 glioblastoma cells either with MV-EGFP, MV-EGFP<sup>miR7</sup>, or MV-EGFP<sup>miR7rc</sup> at an MOI of 0.03. All viruses were able to infect and fuse U87 glioblastoma cells without any difference between the modified viruses and the unmodified parental virus in terms of syncytia formation and cell killing (Figure 5a). In the presence of transfected miR7 precursors, fusion and syncytia formation were strongly reduced, but only in infections with MV-EGFP<sup>miR7</sup>, indicating that miR7 expression interferes with replication of this virus. Moreover, on U87 GBM cells no significant differences in cytolytic properties between the unmodified MV-EGFP virus, the miRTS-containing

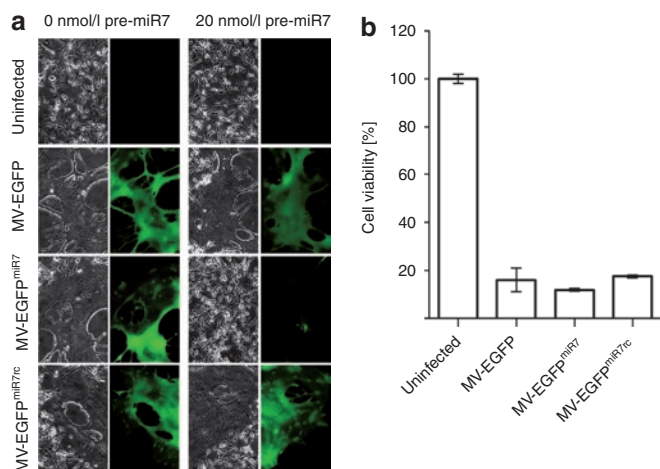


**Figure 5** MV-EGFP<sup>miR7</sup> is highly attenuated in brain-derived cells expressing miR7, but retains full oncolytic activity against glioblastoma cells *in vitro*. **(a)** U87 glioblastoma cells were infected with either control (MV-EGFP, MV-EGFP<sup>miR7rc</sup>) or miR7-sensitive (MV-EGFP<sup>miR7</sup>) virus at a multiplicity of infection (MOI) of 0.03 in the presence or absence of 20 nmol/l pre-miR7. Fluorescence and phase contrast microscopy pictures were taken 50 hours postinfection,  $\times 100$  magnification. **(b)** Cell viability assay of U87 cells infected with different measles virus (MV) variants.  $5 \times 10^4$  U87 cells were either mock-infected or infected with MV-EGFP, MV-EGFP<sup>miR7</sup>, or MV-EGFP<sup>miR7rc</sup> at an MOI of 0.03. 56 hours postinfection, cell viability assay was performed.

MV-EGFP<sup>miR7</sup> and MV-EGFP<sup>miR7rc</sup> viruses in the absence of miR7 could be detected using a cell viability assay (Figure 5b).

### Insertion of microRNA-target elements protects susceptible mice against neuropathogenesis when MV is administered intracerebrally

As an *in vivo* model system to assess this attenuation, we chose the MV-susceptible CD46Ge Ifnar<sup>ko</sup> mice which are susceptible to lethal encephalitis after intracranial challenge with MV.<sup>6,20–22</sup> We injected  $2 \times 10^4$  TCID<sub>50</sub> of either MV-EGFP<sup>miR7</sup> or MV-EGFP<sup>miR7rc</sup> intracranially. Animals receiving MV-EGFP<sup>miR7rc</sup> developed severe signs of neurotoxicity ranging from hypersensitivity to touch and sound, movement and balance difficulties to loss of consciousness. In contrast, none of these symptoms could be detected in mice challenged with miR7-sensitive MV-EGFP<sup>miR7</sup>, indicating that the endogenous expression of miR7 in normal murine brain is sufficient to completely attenuate MV-EGFP<sup>miR7</sup> pathogenesis.

### MicroRNA-sensitive MV-EGFP<sup>miR7</sup> exhibits potent antitumor activity and retains oncolytic efficacy in glioblastoma xenografts

To determine whether expressing microRNA-sensitive elements altered the oncolytic efficacy of MV, we assessed oncolytic potency of miR7-sensitive MV-EGFP<sup>miR7</sup> in glioblastoma xenografts compared to mock infection or infection with parental MV-EGFP. We implanted tumors with  $2 \times 10^6$  U87 glioblastoma cells subcutaneously into the right flank of 6–8 weeks old, female NOD/SCID mice. When the tumors reached an average volume of  $\sim 75 \mu\text{l}$  (at day 4 postimplantation), we either mock-infected the tumors or injected  $8 \times 10^5$  infectious units of MV-EGFP or MV-EGFP<sup>miR7</sup> intratumorally. A total of five injections on consecutive days were

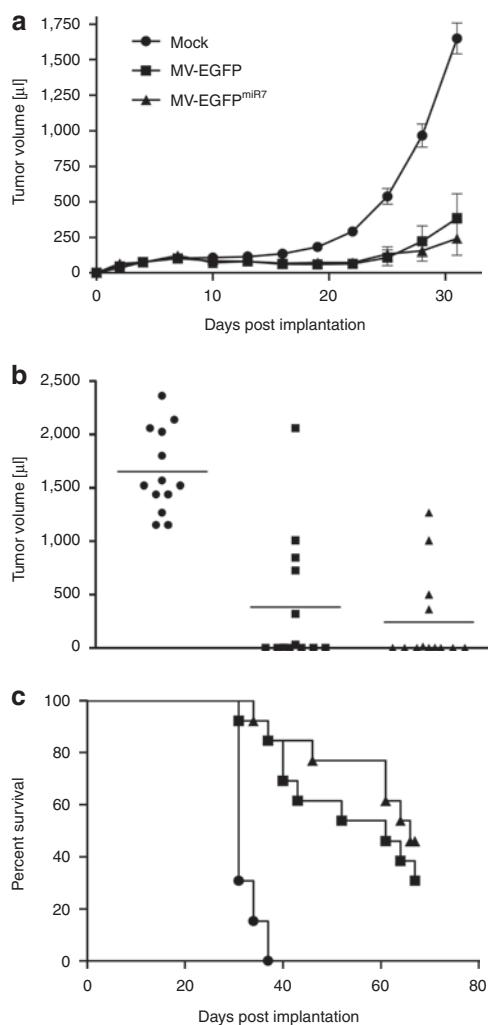


**Figure 6** MV-EGFP<sup>miR7</sup> exhibits potent antitumor activity *in vivo* and retains full efficacy against U87 glioblastoma xenografts despite the insertion of miR7 target sequences. **(a)** Tumor volume measurements starting at day 3 postimplantation. For determination of oncolytic efficacy,  $2 \times 10^6$  U87 glioblastoma cells were subcutaneously implanted into the right flank of 6–8 weeks old, female NOD/SCID mice ( $n = 13/\text{group}$ ). When tumors reached an average volume of  $75 \mu\text{l}$ , they were injected with  $100 \mu\text{l}$  OptiMEM (mock, closed circle) or  $8 \times 10^5$  infectious units of MV-EGFP (closed square), or MV-EGFP<sup>miR7</sup> (closed triangle) on 5 consecutive days. Tumors were measured every third day (starting from the day of implantation). When tumors reached a volume of  $>1,500 \mu\text{l}$ , mice were sacrificed by cervical dislocation. Dots represent mean volume of all animals with error bars based on SE of mean ( $\pm$ SEM). **(b)** Dot plot of the experiment on day 31 postimplantation. **(c)** Corresponding Kaplan–Meier survival plot based on a defined end point of  $>1,500 \mu\text{l}$  tumor volume.

applied and tumor diameters were measured every third day. A similar oncolytic effect with strongly retarded tumor growth compared to mock controls was documented after treatment with both MV-EGFP and MV-EGFP<sup>miR7</sup> (Figure 6a). At day 31, which was the last day with all animals alive, the mean tumor volume in the control group was  $1,650 \mu\text{l}$ , whereas mean tumor volume in both treatment groups was  $<400 \mu\text{l}$  ( $P < 0.0001$ , two-sample *t*-test). Moreover, 6 out of 13 animals treated with MV-EGFP and 7 out of 13 animals treated with MV-EGFP<sup>miR7</sup> showed complete tumor remission at day 31 (Figure 6b). Survival benefits are illustrated

using Kaplan–Meier survival curves with a defined end point of  $>1,500\mu\text{l}$  tumor volume (Figure 6c). Administration of both MV-EGFP and MV-EGFP<sup>miR7</sup> resulted in a significant prolongation of median survival compared to mock therapy ( $P < 0.0001$ , log-rank test). On average 50% of all animals treated with MV had no detectable tumor at day 31, whereas all mock-treated animals had tumors of  $>1,150\mu\text{l}$ . This demonstrates that microRNA-sensitive MV-EGFP<sup>miR7</sup> retains full oncolytic efficacy compared to the unmodified MV vaccine strain *in vivo* in human glioblastoma xenografts with low miR7 expression.

### MicroRNA-sensitive MV-EGFP<sup>miR7</sup> is strongly attenuated in primary human brain explants

To determine whether miR7-sensitive MV-EGFP<sup>miR7</sup> is attenuated in primary human brain tissue physiologically expressing miR7, we obtained normal human brain explants from the invasion front of a resected glioma. The tissue was cut instantly into tissue slices ( $300\mu\text{m}$  thickness) and infected with MV-EGFP, MV-EGFP<sup>miR7</sup>, MV-EGFP<sup>miR7rc</sup>, or mock-infected. As can be seen in Figure 7a, microRNA-sensitive MV-EGFP<sup>miR7</sup> is strongly attenuated in terms of viral transduction and spread compared to control viruses. H/E stained sections of the same brain tissue block were analyzed and displayed brain tissue of the cortex and white matter without morphological signs of malignant transformations (Figure 7b–d).

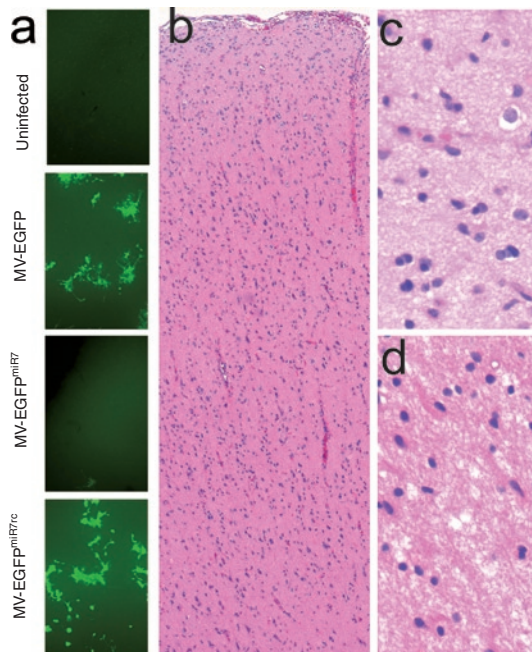


**Figure 7** MV-EGFP<sup>miR7</sup> is attenuated in human brain explants. **(a)** Primary human brain material directly obtained from surgical resection was cut instantly into tissue slices ( $300\mu\text{m}$  thickness) and infected with  $3 \times 10^5$  infectious units of MV-EGFP, MV-EGFP<sup>miR7</sup>, MV-EGFP<sup>miR7rc</sup>, or mock-treated. Fluorescence microscopy was performed 64 hours postinfection. **(b)** H/E staining of primary human brain tissue (overview,  $\times 10$  magnification). The cerebral neocortex from the meninges to the white matter is shown without any morphological signs of malignant transformation. **(c)** H/E stained primary human brain tissue (neocortex),  $\times 100$  magnification. **(d)** H/E stained primary human brain tissue (white matter),  $\times 100$  magnification.

## DISCUSSION

This study demonstrates that microRNA-targeting techniques can be adapted to oncolytic MV for tissue-specific vector tropism and gene expression, increasing the safety profile of MV by tightly restricting replication in normal tissue but not compromising oncolytic potency in target tumor cells.

Based on the Edmonston-B vaccine strain, oncolytic MV has emerged as an excellent candidate for genetic vector engineering to generate armed, targeted, and shielded oncolytics.<sup>23,24</sup> MV has shown potent activity against a variety of preclinical tumor models including colorectal cancer,<sup>25</sup> hepatocellular cancer,<sup>26</sup> pancreatic cancer,<sup>27</sup> prostate cancer,<sup>28</sup> ovarian cancer,<sup>29</sup> breast cancer,<sup>30</sup> mesothelioma,<sup>31</sup> lymphoma,<sup>6,8</sup> myeloma,<sup>32,33</sup> medulloblastoma,<sup>34</sup> and glioma.<sup>35–37</sup> In addition, three different clinical trials using recombinant oncolytic MV have been initiated, including phase I studies for treatment of ovarian cancer, myeloma, and recurrent glioma.<sup>38</sup> However, for next-generation MV vectors, novel strategies to further elevate the therapeutic index by increasing virus safety without perturbing oncolytic activity are still desirable. Although all current clinical trials rely on MV vectors with unmodified tropism, MV vectors with tighter tumor-selectivity could be more confidently paired with chemotherapeutic immunosuppression to increase efficacy in future clinical trials, especially in the most sensitive tissues like brain.

Here, we have shown for the first time that it is possible to engineer microRNA-target sequences into the genome of MV, rendering the virus sensitive to the cognate microRNA. The differential expression of microRNAs in neoplastic tissues is an emerging hallmark of cancer. By choosing microRNAs specifically lost during malignant transformation, tumor specificity can be achieved. This approach has been proven to be feasible for different oncolytic viruses including coxsackie-,<sup>10</sup> adeno-,<sup>13</sup> vesicular stomatitis-,<sup>9,11</sup> and herpes simplex<sup>12</sup> virus. Here, we have demonstrated that this novel postentry targeting technique can be readily adapted to oncolytic MV, thereby adding a new tool to the MV engineering tool box.

In this study, we have focused on miR7, a microRNA mainly expressed in neuronal tissues.<sup>39,40</sup> miR7 is known to regulate the epidermal growth factor receptor and, most importantly, was shown to be downregulated in glioblastoma cells while maintaining high expression levels in surrounding brain tissue.<sup>14,15</sup> Moreover, sequence identity of mature miR7 is fully conserved between mouse and man. Here, we exploited differential expression of this microRNA to enable replication of MV specifically in GBM cells by incorporating synthetic miR7 target sites into the genome. We hypothesized that these sequences would render the associated MV mRNA susceptible to microRNA silencing in nonmalignant, miR7-expressing neurons, but not affect the replication and oncolytic activity of the virus in GBM cells with low miR7 expression. We generated and analyzed oncolytic MV containing multiple target sites for miR7 in the 3'UTR of their F protein genes. We show that this modification efficiently restricts MV spread and progeny production by inhibiting translation of the F protein, strongly reducing viral titers in presence of only 20 nmol/l miR7 precursor molecules. This sensitivity is in the range of other studies in which 50 pmol/l–200 nmol/l microRNAs were used to regulate viral gene expression and replication.<sup>9–11,41</sup> Even though highly attenuated in



the presence of miR7, the virus retained full efficacy against U87 glioblastoma cells *in vitro* and *in vivo*. Both the parental vaccine strain virus and the miR7-sensitive virus significantly retarded the growth of subcutaneously implanted glioblastoma xenografts in NOD/SCID mice and led to a complete remission of the tumor in half of the animals on day 31 postimplantation.

Safety of the virus was demonstrated first after intracranial injection of control and miR7-sensitive virus in MV-susceptible CD46Ge Ifnar<sup>ko</sup> mice. Symptoms of neurotoxicity were seen only in mice receiving control MV, whereas no signs of neurotoxicity were detected in mice challenged with MV-EGFP<sup>miR7</sup>. Second, we demonstrated that physiological expression of miR7 in human brain tissue is sufficient to restrict replication and spread of MV-EGFP<sup>miR7</sup>. This virus was shown to be highly attenuated in fresh human brain explants compared to control virus not bearing miR7 target sites. The results of both experiments indicate an elevated safety level of the miR7 regulated virus.

MV vectors have been successfully engineered to selectively infect certain cell types by displaying specific ligands,<sup>6,23,24,37</sup> often single-chain antibodies, on their hemagglutinin proteins. However, this established entry-level retargeting technique ultimately requires a targetable, unique surface molecule selectively and homogeneously expressed on the surface of the targeted cancer cell type. Even though a variety of these receptors are known, it may occur that cell surface molecules of cancer cells are heterogeneously expressed within the tumor mass and frequently downregulated under selective pressure potentially rendering a subpopulation of target cells insensitive to entry-targeted virotherapy. Thus, in many cases microRNA-targeting can be a valuable alternative or complementary approach to entry-targeted MV.

Besides regulation of viral replication and spread using miRTS, this technique can also be used to shut down expression of non-viral transgenes. MV has shown great utility for delivering therapeutic transgenes to the tumor microenvironment, including *Escherichia coli* purine nucleoside phosphorylase and the human sodium iodide symporter.<sup>5,32</sup> Expression of these transgenes allows the virus to synergize with current clinical therapies, with purine nucleoside phosphorylase activating chemotherapeutics within the tumor microenvironment and sodium iodide symporter leading to uptake of radioactive iodide in infected tumor cells, in both cases leading to bystander killing of uninfected tumor cells. The utility of these approaches relies on accurate tissue-specific expression of the transgenes, especially in the case of sodium iodide symporter, which in addition has the potential to allow precise live-imaging of virus replication. Therefore, tight restriction of transgene expression to tumor cells using microRNA-targeting would benefit both the accuracy of sodium iodide symporter imaging as well as the safety profile of combinatorial virotherapy regimens.

Our findings also suggest that multiple different miRTS could be incorporated into a single MV vector, thereby detargeting several tissues at risk in parallel. This might be of special interest when MV is administered intraperitoneally or intravenously, whereupon the risk of systemic spread and unwanted replication in nontarget tissues is higher than after local administration. Furthermore, the risk of adverse side effects could be minimized when virotherapy is combined with the rational use of chemotherapeutics and immunosuppressors like cyclophosphamide,<sup>8,42,43</sup>

motivating more aggressive future clinical trials without sacrificing rigorous safety standards.

In summary, we have demonstrated that microRNA-targeting can be efficiently adapted to oncolytic MV for tissue-specific vector tropism and gene expression. This new vector engineering tool can now be applied broadly to existing MV vectors for many different therapeutic approaches. Exploiting microRNAs for enhanced tumor-selectivity adds another level of safety to next generation oncolytic MV and elevates their therapeutic index without perturbing their potent oncolytic efficacy.

## MATERIALS AND METHODS

**Construction of plasmids.** For each miRTS, two complementary oligonucleotides with overhanging ends for cloning were generated, hybridized in EB buffer (Qiagen, Hilden, Germany) containing 50 mmol/l NaCl and cloned into the 3'UTR of the MV *F* gene encoded on pCG-F expression vector.<sup>44</sup> All miRTS boxes were designed to be 90 nt total in order to follow the rule of six which is a requirement for MV.<sup>45–47</sup> For cloning, the pCG-F plasmid was *PacI* linearized. Hybridized oligonucleotides with compatible *PvuI*–*PacI* ends were ligated into the linearized vector. The following oligonucleotides were used:

*FmiR7*: 1. 5'-CGACAACAAAATCGCTAGTCTTCCAGAGCTTGA CAACAAAATCGCTAGTCTTCCAGAGCTTGACAACAAAATCGCT AGTCTTCCATTAAT, 2. 5'-TAATGGAAGACTAGCGATTTTGTGTG CAAGCTCTGGAAGACTAGCGATTTTGTGTGCAAGCTCTG GAAGACTAGCGATTTTGTGTGCGAT; *FmiR7rc*: 1. 5'-CGTGAAGA CTAGCGATTTTGTGTGAGCTTGTGGAAGACTAGCGATTTTGT TGTGAGCTTGTGGAAGACTAGCGATTTTGTGTGTTAAT, 2. 5'-TA AACAACAAAATCGCTAGTCTTCCACAAGCTCACAACAAAAT CGCTAGTCTTCCACAAGCTCACAACAAAATCGCT TAGTCTTCCAGAT; *FmiR7mut*: 1. 5'-CGACATCAATTGCGGTA GTCATGCTGAGCTTGACATCAATTGCGGTAAGCTAGTCATGC TGAGCTTGACATCAATTGCGGTAAGCTAGTCTTAAAT, 2. 5'-TAAAG CATGACTACCGCAATTGATGTCAAGCTCAGCATGACTACCGCAA TTGATGTCGAT.

The accuracy of the generated plasmids was verified by single-colony PCR, restriction digest and sequencing. For generation of viral full-length genomic plasmids, the *F* gene of the p(+)MV-EGFP<sup>6,48</sup> plasmid (derived from the Edmonston-B vaccine lineage) was cut out by *NarI*/*PacI* digestion and replaced by the *NarI*/*PacI* digested *F* gene containing the miRTS box. Identity of the genomic plasmids was verified by restriction digest, single-colony PCR, and sequencing.

**Cell culture and viruses.** Vero African green monkey kidney cells and U87 glioblastoma cells were obtained from American Type Culture Collection (ATCC, Manassas, VA). The cells were cultivated in Dulbecco's modified Eagle's medium supplemented with 10% (vol/vol) fetal calf serum at 37°C in a humidified atmosphere of 5% CO<sub>2</sub>. Recombinant MV were generated from complementary DNA constructs according to Radecke *et al.*<sup>45</sup> and subsequently propagated on Vero cells at 37°C. All following infection experiments were performed with viral stocks from the third passage after titer determination.

**Virus titration.** In a 96-well plate, a serial 1:10 dilution of the respective virus in 100 µl medium [DMEM + 10% fetal calf serum (FCS)] per well was done in octuplicates. Thereafter, 1 × 10<sup>4</sup> Vero cells in 100 µl medium were added to each well. Forty-eight hours postinfection (p.i.), individual syncytia in all wells of the appropriate dilution step were counted, and the viral titer (infectious units/ml) was calculated.

**RT-PCR.** Viral genomic RNA from virus stocks was isolated using the Viral RNA Mini Kit (Qiagen) according to the manufacturer's

instructions. First-strand complementary DNA was generated with MV-specific Id-1 (5'-ACCAAACAAGTTGGGTAAGGATAGT-3') and F-5595 (5'-GACTCGTTCCAGCCATCAATCAT-3') primers using the Superscript III First-Strand Synthesis System (Invitrogen, Carlsbad, CA). For PCR-based amplification of the miR7 miRTS box, the F-6747 (5'-CAAGTCGGGAGCAGGAGGTATC-3') and H-7583+ (5'-GGCCAC TTCATCACCGATGATT-3') primers were used. PCR was conducted using the Expand High-Fidelity plus PCR System (Roche, Basel, Switzerland) with the conditions (30 cycles): 15 seconds at 94°C, 30 seconds at 62°C, 120 seconds at 72°C. PCR products were purified using the PCR Purification Kit (Qiagen) and subsequently verified by sequencing.

**MicroRNA precursor transfection.** miR7 precursor molecules (hsa-miR7) were purchased from Ambion (Austin, TX). miRBase accession number: MI0000263. Precursor molecules were transfected at a final concentration of 20 nmol/l using Lipofectamine 2000 (Invitrogen) according to the manufacturer's protocol.

**Fusion assay.**  $2 \times 10^5$  Vero cells cultured in 12-well plates were co-transfected with 0 or 20 nmol/l pre-miR7 (Ambion) and 800 ng each pEGFP-N1 (Clontech, Mountain View, CA) and pCG-F/-H variants using 4  $\mu$ l Lipofectamine 2000 (Invitrogen) per well. As a no-fusion negative control, we transfected only unmodified pCG-F plasmid (along with the pEGFP-N1 reporter plasmid and empty plasmid vector to ensure equal DNA amounts); as a fusion positive control, unmodified pCG-F + pCG-H was transfected (plus pEGFP-N1). Pictures were taken 14 hours post-transfection (p.tr.).

**Virus infection.** Cell culture medium was aspirated and replaced by OptiMEM (Invitrogen) containing viral particles at the indicated MOI. The cells were subsequently incubated at 37°C in a humidified atmosphere of 5% CO<sub>2</sub> for 2 hours and were gently shaken every 15 minutes. Afterwards, virus solution was aspirated and the cells were washed twice with phosphate-buffered saline (PBS). Thereafter, medium (DMEM + 10% FCS) was added and the cells were cultivated as described above.

**Infection +/- miR7.**  $6 \times 10^5$  Vero cells (in 6-well plates) were transfected with 0 or 20 nmol/l miR7 precursors (Ambion) using 8  $\mu$ l Lipofectamine 2000 (Invitrogen) per well. Four hours p.tr., cells were infected with MV-EGFP<sup>miR7</sup>/-miR7<sup>rc</sup> virus at an MOI of 0.03. Cells were incubated at 37°C and pictures were taken 40 hours p.i.

**Immunoblotting.** Fusion assay or infection +/- miR7 was performed as described above. Sixteen hours p.tr. (fusion assay) or 40 hours p.i., cells were washed three times with D-PBS and lysed in 250  $\mu$ l (6-well) lysis buffer [50 mmol/l Tris pH 8.0, 62.5 mmol/l EDTA, 1% Igepal (NP-40), 0.4% deoxycholate, 1 mmol/l phenylmethylsulfonyl fluoride, Complete Protease Inhibitor Cocktail Tablets (Roche) in double-distilled H<sub>2</sub>O]. Cells were scraped, centrifuged for 10 minutes at 1,500g (4°C) and the supernatant was mixed 1:1 with Laemmli buffer [950  $\mu$ l Laemmli sample buffer + 50  $\mu$ l 2-mercaptoethanol (both BioRad, Hercules, CA)]. Samples were denatured for 5 minutes at 95°C, and applied to sodium dodecyl sulfate-polyacrylamide gel electrophoresis [12.5% Criterion gel in 1 $\times$  Tris/Glycin/SDS buffer (BioRad)] for 90 minutes at 130 V. Protein samples were blotted (semidry, 180 mA, 60 minutes) onto PVDF membranes (Immobilon P; Millipore, Bedford, MA) which were then blocked over night at 4°C in 5% dry milk in PBST and incubated with primary anti-F or anti-H (1:5,000) cytoplasmic tail rabbit antibodies<sup>49</sup> or anti-N 505 (1:6,000) rabbit antibody<sup>50</sup> (in blocking buffer) for 1.5 hours at room temperature. After subsequent washing steps, incubation with anti-rabbit horseradish peroxidase-conjugated secondary antibody (1:7,500) or anti- $\beta$ -actin-peroxidase (1:20,000) mouse antibody (A3854; Sigma-Aldrich, St Louis, MO) in blocking buffer was performed for 60 minutes at room temperature. Membranes were then washed and incubated in horseradish peroxidase substrate buffer (SuperSignal West Dura Extended Duration Substrate; Pierce, Rockford,

IL) for 2 minutes followed by exposition to a chemiluminescence film (Kodak Biomax; Kodak, Rochester, MN).

**Virus growth curves.** U87 cells were seeded at a density of  $1 \times 10^5$  cells/well in medium (DMEM + 10% FCS) in 12-well plates. After 6 hours, the respective virus was added at an MOI of 3 (one-step growth curve) or MOI 0.03 (multistep growth curve). Plates were incubated for 2 hours at 37°C in a humidified atmosphere of 5% CO<sub>2</sub> and gently shaken every 15 minutes. Thereafter, cells were washed twice with D-PBS and medium was added. At the designated time points (duplicates), cells were scraped in medium and applied to one freeze-thaw cycle. Samples were vortexed vigorously and centrifuged at 4,000g for 5 minutes at 4°C. Supernatants were collected, equally adjusted to 1 ml volume using DMEM + 10% FCS and directly used for serial-dilution titer determination.

**Cell viability assay (XTT).** U87 cells ( $5 \times 10^4$  per well) cultured in 24-well plates were infected with MV-EGFP, MV-EGFP<sup>miR7</sup>, or MV-EGFP<sup>miR7rc</sup> at an MOI of 0.03, cultured for 156 hours and subsequently measured using the Cell Viability Kit III (PromoKine, Heidelberg, Germany) according to the manufacturer's instructions. For the XTT assay in presence or absence of miR7, Vero cells ( $5 \times 10^4$  per well cultured in 24 well plates) were transfected with 0 or 20 nmol/l miR7 precursor molecules (Ambion) using 2  $\mu$ l Lipofectamine 2000 (Invitrogen) per well. Cells were infected 6.5 hours p.tr. with MV-EGFP<sup>miR7</sup> or MV-EGFP<sup>miR7rc</sup> virus (except for mock-infected control). Cell viability was measured 87 hours p.i. using the Cell Viability Kit III (PromoKine).

**Progeny virus production +/- miR7.** Vero cells were seeded in 12-well plates at a density of  $1.5 \times 10^5$  cells/well in DMEM + 10% FCS. After 4 hours, cells were transfected with 0 or 20 nmol/l pre-miR7 using 4  $\mu$ l Lipofectamine 2000 (Invitrogen). Fifteen hours later, medium was aspirated and the MV-EGFP<sup>miR7</sup>/-miR7<sup>rc</sup> virus was added in 250  $\mu$ l OptiMEM (Invitrogen) at an MOI of 0.03. After 2 hours of adsorption, the virus solution was discarded, cells were washed three times with D-PBS (Invitrogen) and DMEM + 10% FCS was added. After incubation at 37°C for 48 hours, the infected cell layer was scraped in 1 ml OptiMEM, frozen in liquid nitrogen, briefly thawed, vortexed, and centrifuged at 4,000g for 4 minutes to pellet cell debris. The supernatant was stored at -80°C until titration.

**Infection of glioblastoma cells.**  $1 \times 10^5$  U87 glioblastoma cells (in 12-wells) were transfected with either 0 or 20 nmol/l pre-miR7 using 4  $\mu$ l Lipofectamine 2000. Four hours p.tr., cells were infected with unmodified control (MV-EGFP), miR7-responsive (MV-EGFP<sup>miR7</sup>), or miR7-unresponsive (MV-EGFP<sup>miR7rc</sup>) virus at an MOI of 0.03. Cells were incubated at 37°C and pictures were taken 40 hours p.i.

**In vivo experiments for assessment of efficacy.** All animal experimental procedures were performed according to the German Cancer Research Center's animal care guidelines.  $2 \times 10^6$  U87 glioblastoma cells were subcutaneously implanted into the right flank of 6–8 weeks old, female NOD/SCID mice (Harlan, Indianapolis, IN). When tumors reached an average volume of 75  $\mu$ l (day 4 postimplantation), they were injected with 100  $\mu$ l OptiMEM (mock) or  $8 \times 10^5$  infectious units of MV-EGFP or MV-EGFP<sup>miR7</sup> on 5 consecutive days ( $4 \times 10^6$  infectious units in total). Tumors were measured every third day (starting from the day of implantation) using a caliper. The volume of each tumor was calculated with the following formula: (largest diameter  $\times$  smallest diameter<sup>2</sup>)  $\times$  0.5. When tumors reached a volume of >1,500  $\mu$ l, mice were sacrificed by cervical dislocation.

**In vivo experiments for assessment of safety.** All animal experimental procedures were approved by the Mayo Clinic Institutional Animal Care and Use Committee. Intracranial injections were performed as previously described.<sup>6</sup> Briefly,  $2 \times 10^4$  infectious units of either MV-EGFP<sup>miR7</sup> or MV-EGFP<sup>miR7rc</sup> diluted in 20  $\mu$ l OptiMEM (Invitrogen) were injected into the right brain hemisphere of 8-weeks old, transgenic Ifnar<sup>ko</sup>



CD46Ge mice under transient isoflurane anesthesia using an intradermal needle and a Hamilton syringe. Both experimental groups consisted of two animals.

**Infection of primary human brain material.** Patient's informed consent was obtained according to the research proposals approved by the institutional review board at Heidelberg Medical Faculty. Primary human brain tissue from the peripheral invasion front of a glioma resection was obtained from the Department of Neurosurgery, Heidelberg University, and sectioned (300 µm thickness) using a vibratom. The sections were instantly used for *in vitro* infection experiments, and fixed in 4% formalin, paraffin-embedded, sectioned, H/E-stained and analyzed by the Department of Pathology, Heidelberg University. For the infection experiments, the sections were cultivated using cell culture inserts for 6-wells (3.0 µm; BD Biosciences, Franklin Lakes, NJ). Sections were infected with  $1.5 \times 10^5$  infectious units in DMEM 10% FCS + kanamycin (50 µg/ml; Sigma-Aldrich). Medium was exchanged daily and imaging was performed 64 hours p.i.

## SUPPLEMENTARY MATERIAL

**Figure S1.** Insertion of different microRNA-target site (miRTS) boxes does not alter viral replication kinetics.

## ACKNOWLEDGMENTS

We thank Katharina Genreith, Jessica Albert, and Christine Engeland for their valuable technical assistance, Christoph Springfeld and Martin Singh for their careful review of the manuscript, Christel Herold-Mende for providing the human brain material, Wilfried Roth for his support regarding histological analyses and the Light Microscopy Facility at the German Cancer Research Center including Manuela Brom and Felix Bestvater. This work was supported by Deutsche Krebshilfe, German Cancer Aid, Max Eder Program No. 108307 (to G.U.), NIH grant R01 CA139389 (to R.C.), and a Helmholtz Association PhD stipend (to M.F.L.). This work was done in Heidelberg (Germany) and Rochester, MN (USA). Patent applications on which R.C. is an inventor have been licensed to NISCO Inc.; Mayo has an equity position in NISCO; Mayo has not yet received royalties from products developed by the company, but may receive these in the future. All other authors declared no conflict of interest.

## REFERENCES

- Galanis, E, Hartmann, LC, Cliby, WA, Long, HJ, Peethambaram, PP, Barrette, BA *et al.* (2010). Phase I trial of intraperitoneal administration of an oncolytic measles virus strain engineered to express carcinoembryonic antigen for recurrent ovarian cancer. *Cancer Res* **70**: 875–882.
- Liu, TC, Galanis, E and Kim, D (2007). Clinical trial results with oncolytic virotherapy: a century of promise, a decade of progress. *Nat Clin Pract Oncol* **4**: 101–117.
- Myers, R, Harvey, M, Kaufmann, TJ, Greiner, SM, Krempski, JW, Raffel, C *et al.* (2008). Toxicology study of repeat intracerebral administration of a measles virus derivative producing carcinoembryonic antigen in rhesus macaques in support of a phase I/II clinical trial for patients with recurrent gliomas. *Hum Gene Ther* **19**: 690–698.
- Allen, C, Paraskevavou, G, Liu, C, Iankov, ID, Msaouel, P, Zollman, P *et al.* (2008). Oncolytic measles virus strains in the treatment of gliomas. *Expert Opin Biol Ther* **8**: 213–220.
- Ungerechts, G, Springfeld, C, Frenzke, ME, Lampe, J, Parker, WB, Sorscher, EJ *et al.* (2007). An immunocompetent murine model for oncolysis with an armed and targeted measles virus. *Mol Ther* **15**: 1991–1997.
- Ungerechts, G, Springfeld, C, Frenzke, ME, Lampe, J, Johnston, PB, Parker, WB *et al.* (2007). Lymphoma chemovirotherapy: CD20-targeted and convertase-armed measles virus can synergize with fludarabine. *Cancer Res* **67**: 10939–10947.
- Fulci, G, Breyman, L, Gianni, D, Kurozumi, K, Rhee, SS, Yu, J *et al.* (2006). Cyclophosphamide enhances glioma virotherapy by inhibiting innate immune responses. *Proc Natl Acad Sci USA* **103**: 12873–12878.
- Ungerechts, G, Frenzke, ME, Yaiw, KC, Miest, T, Johnston, PB and Cattaneo, R (2010). Mantle cell lymphoma salvage regimen: synergy between a reprogrammed oncolytic virus and two chemotherapeutics. *Gene Ther* **17**: 1506–1516.
- Edge, RE, Falls, TJ, Brown, CW, Lichty, BD, Atkins, H and Bell, JC (2008). A let-7 MicroRNA-sensitive vesicular stomatitis virus demonstrates tumor-specific replication. *Mol Ther* **16**: 1437–1443.
- Kelly, EJ, Hadac, EM, Greiner, S and Russell, SJ (2008). Engineering microRNA responsiveness to decrease virus pathogenicity. *Nat Med* **14**: 1278–1283.
- Kelly, EJ, Nace, R, Barber, GN and Russell, SJ (2010). Attenuation of vesicular stomatitis virus encephalitis through microRNA targeting. *J Virol* **84**: 1550–1562.
- Lee, CY, Rennie, PS and Jia, WW (2009). MicroRNA regulation of oncolytic herpes simplex virus-1 for selective killing of prostate cancer cells. *Clin Cancer Res* **15**: 5126–5135.
- Ylösmäki, E, Hakkarainen, T, Hemminki, A, Visakorpi, T, Andino, R and Saksela, K (2008). Generation of a conditionally replicating adenovirus based on targeted destruction of E1A mRNA by a cell type-specific MicroRNA. *J Virol* **82**: 11009–11015.
- Kefas, B, Godlewski, J, Comeau, L, Li, Y, Abounader, R, Hawkinson, M *et al.* (2008). microRNA-7 inhibits the epidermal growth factor receptor and the Akt pathway and is down-regulated in glioblastoma. *Cancer Res* **68**: 3566–3572.
- Webster, RJ, Giles, KM, Price, KJ, Zhang, PM, Mattick, JS and Leedman, PJ (2009). Regulation of epidermal growth factor receptor signaling in human cancer cells by microRNA-7. *J Biol Chem* **284**: 5731–5741.
- Landgraf, P, Rusu, M, Sheridan, R, Sewer, A, Iovino, N, Aravin, A *et al.* (2007). A mammalian microRNA expression atlas based on small RNA library sequencing. *Cell* **129**: 1401–1414.
- Bourhis, JM, Canard, B and Longhi, S (2006). Structural disorder within the replicative complex of measles virus: functional implications. *Virology* **344**: 94–110.
- Leonard, VH, Hodge, G, Reyes-Del Valle, J, McChesney, MB and Cattaneo, R (2010). Measles virus selectively blind to signaling lymphocytic activation molecule (SLAM; CD150) is attenuated and induces strong adaptive immune responses in rhesus monkeys. *J Virol* **84**: 3413–3420.
- Leonard, VH, Sinn, PL, Hodge, G, Miest, T, Devaux, P, Oezguen, N *et al.* (2008). Measles virus blind to its epithelial cell receptor remains virulent in rhesus monkeys but cannot cross the airway epithelium and is not shed. *J Clin Invest* **118**: 2448–2458.
- Springfeld, C, von Messling, V, Frenzke, M, Ungerechts, G, Buchholz, CJ and Cattaneo, R (2006). Oncolytic efficacy and enhanced safety of measles virus activated by tumor-secreted matrix metalloproteinases. *Cancer Res* **66**: 7694–7700.
- Cathomen, T, Mrkic, B, Spehner, D, Drilien, R, Naef, R, Pavlovic, J *et al.* (1998). A matrix-less measles virus is infectious and elicits extensive cell fusion: consequences for propagation in the brain. *EMBO J* **17**: 3899–3908.
- Duprex, WP, McQuaid, S, Roscic-Mrkic, B, Cattaneo, R, McCallister, C and Rima, BK (2000). *In vitro* and *in vivo* infection of neural cells by a recombinant measles virus expressing enhanced green fluorescent protein. *J Virol* **74**: 7972–7979.
- Cattaneo, R, Miest, T, Shashkova, EV and Barry, MA (2008). Reprogrammed viruses as cancer therapeutics: targeted, armed and shielded. *Nat Rev Microbiol* **6**: 529–540.
- Cattaneo, R (2010). Paramyxovirus entry and targeted vectors for cancer therapy. *PLoS Pathog* **6**: e1000973.
- Hoffmann, D, Bangen, JM, Bayer, W and Wildner, O (2006). Synergy between expression of fusogenic membrane proteins, chemotherapy and facultative virotherapy in colorectal cancer. *Gene Ther* **13**: 1534–1544.
- Blechacz, B, Splinter, PL, Greiner, S, Myers, R, Peng, KW, Federspiel, MJ *et al.* (2006). Engineered measles virus as a novel oncolytic viral therapy system for hepatocellular carcinoma. *Hepatology* **44**: 1465–1477.
- Penheiter, AR, Wegman, TR, Classic, KL, Dingli, D, Bender, CE, Russell, SJ *et al.* (2010). Sodium iodide symporter (NIS)-mediated radiovirotherapy for pancreatic cancer. *AJR Am J Roentgenol* **195**: 341–349.
- Msaouel, P, Iankov, ID, Allen, C, Morris, JC, von Messling, V, Cattaneo, R *et al.* (2009). Engineered measles virus as a novel oncolytic therapy against prostate cancer. *Prostate* **69**: 82–91.
- Peng, KW, TenEyck, CJ, Galanis, E, Kalli, KR, Hartmann, LC and Russell, SJ (2002). Intraperitoneal therapy of ovarian cancer using an engineered measles virus. *Cancer Res* **62**: 4656–4662.
- McDonald, CJ, Erlichman, C, Ingle, JN, Rosales, GA, Allen, C, Greiner, SM *et al.* (2006). A measles virus vaccine strain derivative as a novel oncolytic agent against breast cancer. *Breast Cancer Res Treat* **99**: 177–184.
- Li, H, Peng, KW, Dingli, D, Kratzke, RA and Russell, SJ (2010). Oncolytic measles viruses encoding interferon beta and the thyroidal sodium iodide symporter gene for mesothelioma virotherapy. *Cancer Gene Ther* **17**: 550–558.
- Dingli, D, Peng, KW, Harvey, ME, Greipp, PR, O'Connor, MK, Cattaneo, R *et al.* (2004). Image-guided radiovirotherapy for multiple myeloma using a recombinant measles virus expressing the thyroidal sodium iodide symporter. *Blood* **103**: 1641–1646.
- Munguia, A, Ota, T, Miest, T and Russell, SJ (2008). Cell carriers to deliver oncolytic viruses to sites of myeloma tumor growth. *Gene Ther* **15**: 797–806.
- Studebaker, AW, Kreofsky, CR, Pierson, CR, Russell, SJ, Galanis, E and Raffel, C (2010). Treatment of medulloblastoma with a modified measles virus. *Neuro-oncology* **12**: 1034–1042.
- Allen, C, Vongpunsawad, S, Nakamura, T, James, CD, Schroeder, M, Cattaneo, R *et al.* (2006). Retargeted oncolytic measles strains entering via the EGFRvIII receptor maintain significant antitumor activity against gliomas with increased tumor specificity. *Cancer Res* **66**: 11840–11850.
- Paraskevavou, G, Allen, C, Nakamura, T, Zollman, P, James, CD, Peng, KW *et al.* (2007). Epidermal growth factor receptor (EGFR)-retargeted measles virus strains effectively target EGFR- or EGFRvIII expressing gliomas. *Mol Ther* **15**: 677–686.
- Allen, C, Paraskevavou, G, Iankov, I, Giannini, C, Schroeder, M, Sarkaria, J *et al.* (2008). Interleukin-13 displaying retargeted oncolytic measles virus strains have significant activity against gliomas with improved specificity. *Mol Ther* **16**: 1556–1564.
- Russell, SJ and Peng, KW (2009). Measles virus for cancer therapy. *Curr Top Microbiol Immunol* **330**: 213–241.
- Junn, E, Lee, KW, Jeong, BS, Chan, TW, Im, JY and Mouradian, MM (2009). Repression of alpha-synuclein expression and toxicity by microRNA-7. *Proc Natl Acad Sci USA* **106**: 13052–13057.
- Doxakis, E (2010). Post-transcriptional regulation of alpha-synuclein expression by mir-7 and mir-153. *J Biol Chem* **285**: 12726–12734.
- Kelly, EJ, Hadac, EM, Cullen, BR and Russell, SJ (2010). MicroRNA antagonism of the picornaviral life cycle: alternative mechanisms of interference. *PLoS Pathog* **6**: e1000820.
- Myers, RM, Greiner, SM, Harvey, ME, Griesmann, G, Kuffel, MJ, Buhrow, SA *et al.* (2007). Preclinical pharmacology and toxicology of intravenous MV-NIS, an oncolytic measles virus administered with or without cyclophosphamide. *Clin Pharmacol Ther* **82**: 700–710.

43. Lun, XQ, Jang, JH, Tang, N, Deng, H, Head, R, Bell, JC *et al.* (2009). Efficacy of systemically administered oncolytic vaccinia virotherapy for malignant gliomas is enhanced by combination therapy with rapamycin or cyclophosphamide. *Clin Cancer Res* **15**: 2777–2788.
44. Cathomen, T, Naim, HY and Cattaneo, R (1998). Measles viruses with altered envelope protein cytoplasmic tails gain cell fusion competence. *J Virol* **72**: 1224–1234.
45. Radecke, F, Spielhofer, P, Schneider, H, Kaelin, K, Huber, M, Dötsch, C *et al.* (1995). Rescue of measles viruses from cloned DNA. *EMBO J* **14**: 5773–5784.
46. Calain, P and Roux, L (1993). The rule of six, a basic feature for efficient replication of Sendai virus defective interfering RNA. *J Virol* **67**: 4822–4830.
47. Rager, M, Vongpunsawad, S, Duprex, WP and Cattaneo, R (2002). Polyploid measles virus with hexameric genome length. *EMBO J* **21**: 2364–2372.
48. Duprex, WP, McQuaid, S, Hangartner, L, Billeter, MA and Rima, BK (1999). Observation of measles virus cell-to-cell spread in astrocytoma cells by using a green fluorescent protein-expressing recombinant virus. *J Virol* **73**: 9568–9575.
49. Mühlebach, MD, Leonard, VH and Cattaneo, R (2008). The measles virus fusion protein transmembrane region modulates availability of an active glycoprotein complex and fusion efficiency. *J Virol* **82**: 11437–11445.
50. Toth, AM, Devaux, P, Cattaneo, R and Samuel, CE (2009). Protein kinase PKR mediates the apoptosis induction and growth restriction phenotypes of C protein-deficient measles virus. *J Virol* **83**: 961–968.